# Electron spin relaxation of N@C$_{60}$ in CS$_2$

John J. L. Morton[a)]
*Department of Materials, Oxford University, Oxford OX1 3PH, United Kingdom and Clarendon Laboratory, Department of Physics, Oxford University, Oxford OX1 3PU, United Kingdom*

Alexei M. Tyryshkin
*Department of Electrical Engineering, Princeton University, Princeton, New Jersey 08544*

Arzhang Ardavan
*Clarendon Laboratory, Department of Physics, Oxford University, Oxford OX1 3PU, United Kingdom*

Kyriakos Porfyrakis
*Department of Materials, Oxford University, Oxford OX1 3PH, United Kingdom*

S. A. Lyon
*Department of Electrical Engineering, Princeton University, Princeton, New Jersey 08544*

G. Andrew D. Briggs
*Department of Materials, Oxford University, Oxford OX1 3PH, United Kingdom*

We examine the temperature dependence of the electron spin relaxation times of the molecules N@C$_{60}$ and N@C$_{70}$ (which comprise atomic nitrogen trapped within a carbon cage) in liquid CS$_2$ solution. The results are inconsistent with the fluctuating zero-field splitting (ZFS) mechanism, which is commonly invoked to explain electron spin relaxation for $S \geq 1$ spins in liquid solution, and is the mechanism postulated in the literature for these systems. Instead, we find an Arrhenius temperature dependence for N@C$_{60}$, indicating the spin relaxation is driven primarily by an Orbach process. For the asymmetric N@C$_{70}$ molecule, which has a permanent ZFS, we resolve an additional relaxation mechanism caused by the rapid reorientation of its ZFS. We also report the longest coherence time ($T_2$) ever observed for a molecular electron spin, being 0.25 ms at 170 K. © *2006 American Institute of Physics.* [DOI: 10.1063/1.2147262]

## I. INTRODUCTION

The encapsulation of atomic nitrogen within a fullerene shield has provided a uniquely robust molecular electron spin.[1] Its unique relaxation properties have enabled the observations of a novel type of electron spin-echo envelope modulation[2] (ESEEM) and attracted attention as a potential embodiment of a bit of quantum information.[3]

In high spin systems ($S \geq 1$) in liquid solution, a fluctuating zero-field splitting (ZFS) has habitually been cited as the dominant relaxation mechanism since transition-metal ions were first studied by EPR.[4,5] When relaxation in N@C$_{60}$ (which has electron spin $S=3/2$) was first studied, it was therefore natural to assume that the same ZFS mechanism applied.[6] However, to date there has been little evidence to support this hypothesis. For example, no temperature dependence has been reported for N@C$_{60}$ in solution; such a study is critical in determining unambiguously which relaxation mechanisms are relevant. Measurements have been reported in CS$_2$ and toluene solutions;[7] however, the analysis of these results ignored the effects of magnetic nuclei in toluene, which we have found to contribute significantly to the relaxation.[8] Finally, the previous measurements were performed using fullerene solutions that were sufficiently concentrated for (C$_{60}$)$_n$ aggregates to form, so it is

difficult to conclude which phase (liquid or solid) the reported $T_1/T_2$ times correspond to.[9] Consequently, the favored relaxation model of a ZFS fluctuation has little direct evidence to support it, and must be critically reevaluated.

In this letter we report relaxation times for both N@C$_{60}$ and N@C$_{70}$ in CS$_2$ solution, which, conveniently, lacks nuclear spins in the dominant isotopes of its constituents. We find that the temperature dependence of the relaxation times is inconsistent with the previously proposed ZFS mechanism, and suggest an alternate Orbach relaxation mechanism. We extract an energy gap which matches well the first excited vibrational state of the fullerene cage.

## II. MATERIALS AND METHODS

High-purity endohedral N@C$_{60}$ was prepared,[10] dissolved in CS$_2$ to a final fullerene concentration of $1-2 \times 10^{15}$/cm$^3$, freeze pumped in three cycles to remove oxygen, and finally sealed in a quartz EPR tube. The fullerene concentration used ($\approx 1$ $\mu$M) was well below the cluster formation threshold.[9] Samples were 0.7–1.4 cm long, and contained approximately $5 \times 10^{13}$ N@C$_{60}$ spins. Pulsed EPR measurements were performed using an $X$-band Bruker Elexsys580e spectrometer, equipped with a nitrogen-flow cryostat. $T_2$ and $T_1$ times were measured using two-pulse (Hahn) electron spin echo (ESE) and inversion recovery experiments, respectively. The $\pi/2$ and $\pi$ pulse durations were

---

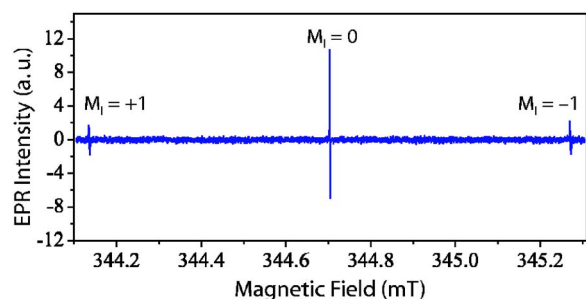a)Electronic mail: john.morton@materials.ox.ac.uk

**124**, 014508-1

FIG. 1. Continuous-wave EPR spectrum of N@C$_{60}$ in CS$_2$ at room temperature. Each line in the triplet signal is labeled with the corresponding projection $M_I$ of the $^{14}$N nuclear spin. Measurement parameters: microwave frequency, 9.67 GHz; microwave power, 0.5 $\mu$W; modulation amplitude, 2 mG; and modulation frequency, 1.6 kHz.

56 and 112 ns, respectively. Phase cycling was used to eliminate the contribution of unwanted free-induction decay (FID) signals.

Figure 1 shows the continuous-wave EPR spectrum of N@C$_{60}$ in CS$_2$ at room temperature. The spectrum is centered on the electron $g$ factor $g = 2.0036$ and comprises three narrow lines (linewidth $<0.3$ $\mu$T) resulting from the hyperfine coupling to $^{14}$N.[11] The relevant isotropic spin Hamiltonian (in angular frequency units) is

$$\mathcal{H}_0 = \omega_e S_z - \omega_I I_z + a \cdot \mathbf{S} \cdot \mathbf{I}, \tag{1}$$

where $\omega_e = g\beta B_0/\hbar$ and $\omega_I = g_I \beta_n B_0/\hbar$ are the electron and $^{14}$N nuclear Zeeman frequencies, $g$ and $g_I$ are the electron and nuclear $g$ factors, $\beta$ and $\beta_n$ are the Bohr and nuclear magnetons, $\hbar$ is Planck's constant and $B_0$ is the magnetic field applied along $z$ axis in the laboratory frame. Each hyperfine line (marked in Fig. 1 with $M_I = 0$ and $\pm 1$) involves the three allowed electron spin transitions $\Delta M_S = 1$ within the $S = 3/2$ multiplet. These electron spin transitions remain degenerate for $M_I = 0$ but split into three lines for $M_I = \pm 1$. This additional splitting of 0.9 $\mu$T originates from the second-order hyperfine corrections and leads to a modulation of the electron spin echo decay.[2]

## III. RELAXATION OF N@C$_{60}$ IN CS$_2$

Spin relaxation times $T_1$ and $T_2$ for N@C$_{60}$ in CS$_2$, measured on the central $M_I = 0$ hyperfine line, are shown on a logarithmic scale in Fig. 2 for a range of temperatures (160–300 K), demonstrating an exponential temperature dependence and a roughly constant ratio $T_2 \approx (2/3)T_1$ over the full temperature range. This contrasts with previous findings which reported no temperature dependence for $T_2$.[3] Below 160 K, the CS$_2$ solvent freezes as a polycrystal, leaving regions of high fullerene concentration around grain boundaries. This dramatically increases the local spin concentration, and $T_2$ becomes extremely short due to dipolar spin coupling (the so-called instantaneous diffusion effect).[12–14]

As this is an $S = 3/2$ spin system, one might expect several different relaxation times corresponding to the different $\Delta M_S = 1$ transitions. However, in the experiments presented in Fig. 2, all decays were well described by monoexponentials. Given two similar exponential decays, it is notoriously difficult to extract anything other than a single, average de-
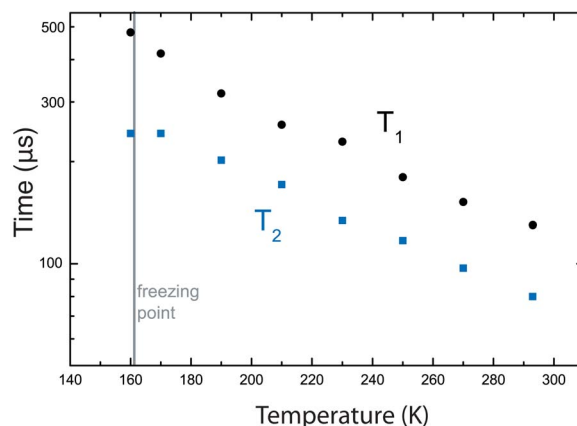


FIG. 2. Electron spin relaxation times ($T_1$ and $T_2$) of N@C$_{60}$ in CS$_2$, measured using the central $M_I = 0$ line. The ratio $T_2 \approx (2/3)T_1$ is maintained over the full temperature range for which the solvent remains liquid.

cay constant from an exponential fit. Here, we take advantage of a recently reported mechanism for ESEEM (Ref. 2) to separate the relaxation times for different electron transitions. This modulation generates an echo intensity for transitions on the $M_I = \pm 1$ lines which varies as a function of the delay time, $\tau$, as

$$V_{M_I = \pm 1}(\tau) = 2 + 3 \cos 2\delta\tau. \tag{2}$$

The oscillating component arises from the "outer" coherences (from the $M_S = \pm 3/2 : \pm 1/2$ transitions), while the unmodulated component arises from the "inner" coherences (from the $M_S = +1/2 : -1/2$ transition). If $T_2$ relaxation is included, Eq. (2) transforms to

$$V_{M_I = \pm 1}(\tau) = 2 \exp(-2\tau/T_{2,i}) + 3 \exp(-2\tau/T_{2,o})\cos 2\delta\tau, \tag{3}$$

where $T_{2,i}$ and $T_{2,o}$ are the relaxation times of the inner and outer coherences, respectively. Thus, by fitting to the modulated ESEEM decay, the individual relaxation times $T_{2,i}$ and $T_{2,o}$ can be extracted. $T_1$ and $T_2$ times measured for the high-field ($M_I = -1$) hyperfine line are shown in Fig. 3. $T_1$ was
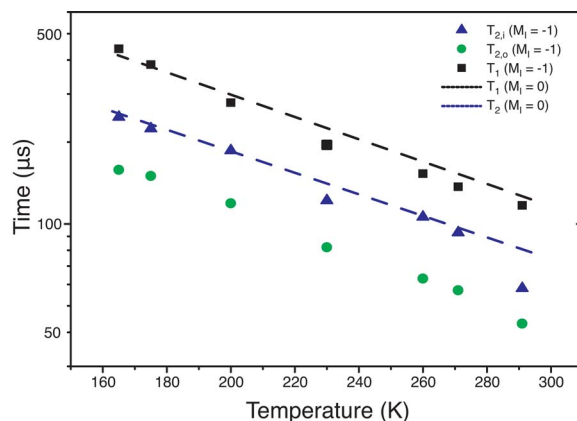


FIG. 3. Electron spin relaxation times ($T_1$ and $T_2$) of N@C$_{60}$ in CS$_2$, measured using the high field $M_I = -1$ line. ESEEM is used to resolve the individual decay rates of the inner and outer coherences [see Eq. (3)]. Dashed curves show corresponding data taken for the central $M_I = 0$ line, for comparison.

measured in the standard way (inversion recovery), and so only one (average) value was obtained.

The behavior of $T_1$ appears identical for both central and high-field lines, indicating that relaxation caused by the hyperfine interaction with the nitrogen nuclear spin is negligible. The $T_{2,i}$ measured on the high-field $M_I=-1$ hyperfine line correlates closely with the $T_2$ measured on the central $M_I=0$ line. Remarkably, both of these $T_2$ times remain approximately 2/3 of $T_1$ over the full temperature range studied. For the high-field line, the ratio of $T_{2,o}$ to $T_{2,i}$ also stays constant at about 2/3. The fact that certain ratios between $T_1$, $T_{2,i}$, and $T_{2,o}$ remain constant over a broad temperature range is a strong indication that all of these relaxation times are limited by the same mechanism. In the following section, we review different relaxation mechanisms which might account for the observed temperature dependence.

## A. ZFS fluctuations

Spin relaxation is manifested in fluctuating terms in the spin Hamiltonian and arises from fluctuating magnetic dipoles (either nuclear or electronic), and other motions causing variations in the interactions between the spin and its environment. The trapping of endohedral nitrogen in a high-symmetry environment suppresses most of the conventional spin-relaxation mechanisms [zero-field splitting (ZFS) interaction, anisotropic $g$ matrix, electron-nuclear dipolar coupling and nuclear quadrupole interaction]. Indeed, it has been proposed that the dominant relaxation process arises from small deviations from this ideal symmetric environment, caused by cage deformations from collisions with solvent molecules.[1] For example, the modulation of the hyperfine interaction through such collisions is a possible relaxation pathway. This was dismissed in earlier reports on the basis that the expected $M_I$ dependence of linewidth that this mechanism predicts is not observed.[1] However, as all linewidths are likely to be instrumentally limited, this observation did not constitute a rigorous confutation.

The mechanism favored in the literature is that of a ZFS fluctuation, again caused by deformation of the spherical C$_{60}$ cage through solvent collisions.[6] Given the concentrations of fullerene solution that were reported in these earlier studies, a large amount of fullerene aggregation is expected[9] and so it is unlikely that the N@C$_{60}$ molecules being studied had any direct contact with solvents. Nevertheless, deformations of the cage, through whichever mechanism (such as collisions with other C$_{60}$ molecules in the cluster), will give rise to some time varying ZFS. Alternatively, ZFS fluctuations may result from rotational tumbling in molecules that have a permanent nonzero ZFS (such as in N@C$_{70}$). In the case of a degenerate $S=3/2$ system, a fluctuating ZFS term leads, in general, to two different decoherence times,[15]

$$(T_{2,i})^{-1} = \frac{4}{5}D_{\text{eff}}^2\left[\frac{\tau_c}{1+\omega_e^2\tau_c^2} + \frac{\tau_c}{1+4\omega_e^2\tau_c^2}\right],\qquad(4)$$

$$(T_{2,o})^{-1} = \frac{4}{5}D_{\text{eff}}^2\left[\tau_c + \frac{\tau_c}{1+\omega_e^2\tau_c^2}\right],\qquad(5)$$

for the transitions that we refer to here as inner and outer, respectively. $D_{\text{eff}}^2 = D^2 + 3E^2$, $D$ and $E$ are the coupling and rhombicity ZFS parameters, $\tau_c$ is the correlation time of the fluctuations, and $\omega_e$ is the electron spin transition frequency.

The predicted $T_1$ times arising form the same mechanism are

$$(T_{1,i})^{-1} = \frac{8}{5}D_{\text{eff}}^2\left[\frac{\tau_c}{1+\omega_e^2\tau_c^2}\right],\qquad(6)$$

$$(T_{1,o})^{-1} = \frac{8}{5}D_{\text{eff}}^2\left[\frac{\tau_c}{1+4\omega_e^2\tau_c^2}\right].\qquad(7)$$

The individual values of $T_{1,i}$ and $T_{1,o}$ cannot be resolved in a simple inversion recovery experiment, and thus only their average can be determined (with respective weights 2 and 3).

In the fast tumbling limit ($\omega_e\tau_c\ll1$), the theory predicts these two $T_1$ times to be identical, and equal to both types of $T_2$, contrary to our observed ratio of 2/3. Moving away from the fast-tumbling limit, the values for $D_{\text{eff}}$ and $\tau_c$ can be derived given any values for $T_1$ and $T_2$. Since the ratio between these times is dictated purely by $\tau_c$, the fact that the ratios stay fixed implies $\tau_c$, the correlation time of the ZFS fluctuations, stays fixed over the broad temperature range (160–300 K). This would be surprising, as the viscosity of CS$_2$ changes by an order of magnitude over this temperature range.[16] Thus, we conclude that the previously suggested ZFS fluctuation mechanism cannot explain the observed temperature dependence of $T_1$ and $T_2$, nor their mutual correlation, and therefore seek alternative explanations for the behavior observed.

## B. Orbach relaxation process

The temperature dependence of $T_1$ is well described by an Orbach relaxation mechanism (see Fig. 4). This is a two-phonon relaxation process whose energies are resonant with a transition to an excited electronic state (i.e., a vibrational or orbital state which lies outside of the space considered by the spin Hamiltonian). The $T_1$ temperature dependence is dictated by the distribution of phonon energies, and is of the form:

$$T_1 = A(e^{\Delta/kT} - 1),\qquad(8)$$

where $\Delta$ is the energy gap to the excited state and $A$ is some constant which involves terms associated with spin-orbit coupling (and therefore with the ZFS, $^{14}$N hyperfine coupling and $g$ tensor in the excited state).[17] A fit to the data in Fig. 4 yields $\Delta=32(1)$ meV. This is a close match to the energy of the first vibrational mode of C$_{60}$ (273 cm$^{-1}$ or 34 meV) which has been theoretically calculated and observed by Raman spectroscopy of C$_{60}$ in CS$_2$ solution at 300 K,[18–20] indicating that this may be a vibrational spin-orbit Orbach process.[21,22] This first excited vibrational mode, termed $H_g(1)$, breaks the spherical symmetry of the molecule, reducing it to axial. The small difference between $\Delta$
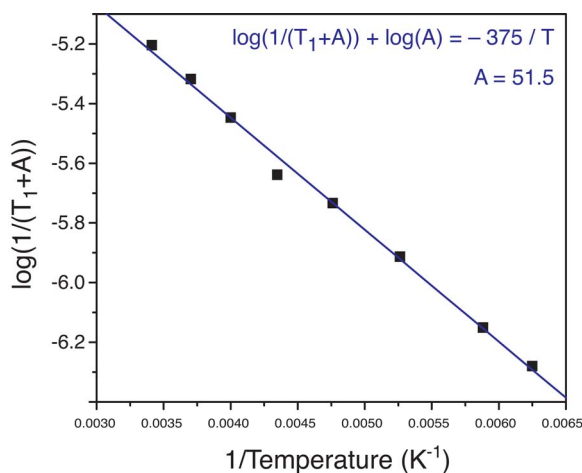
$$\log(1/(T_1+A)) + \log(A) = -375/T$$

$$A = 51.5$$

FIG. 4. The temperature dependence of $T_1$ of N@$C_{60}$ is linear in Arrhenius coordinates, consistent with the Orbach relaxation mechanism. An energy gap $\Delta = 32(1)$ meV $\equiv 375$ K can be extracted. Because we cannot make a low-temperature approximation in this case, the standard Orbach plot of $\log(1/T_1)$ vs $1/T$ must be adjusted to include the constant of proportionality, $A$ [see Eq. (8)]. The plot is then recursively fit to fine-tune $A$ and obtain the slope, $\Delta/k$. $T_1$ is given in microseconds.

observed here compared with that seen in the Raman spectroscopy of $C_{60}$ could be due to a shift in vibrational energies due to the presence of the endohedral nitrogen atom.

The strong correlations observed in the temperature dependence of $T_1$, $T_{2,i}$, and $T_{2,o}$ indicate that the $T_2$ times are also limited by the Orbach mechanism. However, no detailed Orbach theory has been developed for high-spin systems—developing such a theory lies beyond the scope of the current work.

## IV. RELAXATION OF N@$C_{70}$ IN CS$_2$

The Raman spectrum of $C_{70}$ is very similar to that of $C_{60}$, while its rugby ball shape provides a permanent nonzero ZFS to an endohedral spin. N@$C_{70}$ is therefore an ideal candidate to further compare the mechanisms of a vibrational Orbach relaxation with one induced by ZFS fluctuations (here, caused by molecular rotations). Using the methods outlined above, we measured $T_2$ (for both the inner and outer coherences) and $T_1$, shown in Fig. 5.
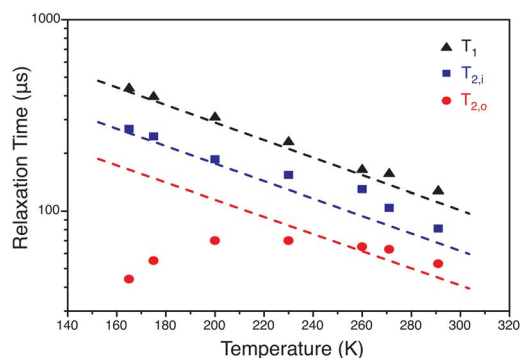


FIG. 5. Temperature dependence of $T_1$ and $T_2$ times for N@$C_{70}$ in CS$_2$. For comparison, dashed lines show linear fits to the corresponding data for N@$C_{60}$ in CS$_2$ (from Fig. 3).

The temperature dependence of $T_1$ is similar to that seen for N@$C_{60}$ in CS$_2$. The first excited vibrational mode of $C_{70}$ is only about 1.7 meV lower in energy than the equivalent mode in $C_{60}$.[23] Consistent with this, the $T_1$ temperature dependence seen for N@$C_{70}$ is slightly weaker than measured on the outer line of N@$C_{60}$, though the difference falls within experimental error.

While $T_{2,i}$ here bears a strong resemblance to that seen for N@$C_{60}$, $T_{2,o}$ for N@$C_{70}$ shows a nonmonotonic temperature dependence, peaking around 230 K. We now show that this behavior can be explained by the presence of the built-in ZFS in N@$C_{70}$, and by the change of rotational mobility of the molecule as the temperature drops. An estimate of the built-in ZFS parameter in N@$C_{70}$ has been reported by aligning the molecules in a liquid crystal, and was found to be $D = 2.5$ MHz (0.8 G).[24] However, due to the uncertainty in the order parameter ($O_{33}$), this value should be considered as a lower limit of the true ZFS parameter. At higher temperatures (i.e., in the fast-tumbling regime) this ZFS is averaged out sufficiently so that all relaxation times are identical to those for N@$C_{60}$. However, upon cooling below 250 K, the viscosity of CS$_2$ rises sharply,[16] thus slowing the N@$C_{70}$ tumbling rate and resulting in incomplete averaging of the ZFS. We simulate this effect using Eqs. (4) and (5) and find that while $T_{2,o}$ is affected by this mechanism, both $T_{2,i}$ and $T_1$ are not.

In this simulation we assume that two relaxation mechanisms are involved. One is the Orbach mechanism which produces the correlations $T_{2,i}/T_1 = T_{2,o}/T_{2,i} = 2/3$ over the full temperature range studied, as observed for N@$C_{60}$. The second is the mechanism due to ZFS fluctuation, described above. The Stokes-Einstein-Debye model,

$$\tau_r = \frac{4\pi\eta a^3}{2kT}, \tag{9}$$

and experimental values for the viscosity of CS$_2$ (Ref. 16) are used to obtain the rotational correlation time, $\tau_r$, as a function of temperature. The effective radius of $C_{70}$ was taken to be 5.4 Å.[25] The experimental data were well fit by this model, using only one fitting parameter, $D$ (given the axial symmetry of $C_{70}$, we assume $E = 0$). The result is shown in Fig. 6, where the best-fit value for $D$ is 5.5 MHz (2 G). This value is large compared with estimates described in the literature,[24] however, it is consistent with values for $D$ measured with other modifications of N@$C_{60}$ [for example, $D$ was measured in N@$C_{60}$O to be 2.4 G (Ref. 26)].

Figure 6 also shows that the ZFS mechanism affects only $T_{2,o}$, and does not produce a noticeable effect on $T_{2,i}$ and $T_1$.

## V. CONCLUSIONS

In summary, we have reported the temperature dependences of electron spin relaxation in nitrogen-doped fullerenes, using ESEEM to resolve the relaxation rates of different coherences of this $S = 3/2$ spin. Our findings are contradictory with the previously suggested mechanism of a fluctuating ZFS, which is often assumed to be the dominant mechanism in all high spin ($S \geq 1$) systems. Instead, the temperature dependences we observe are strongly suggestive of
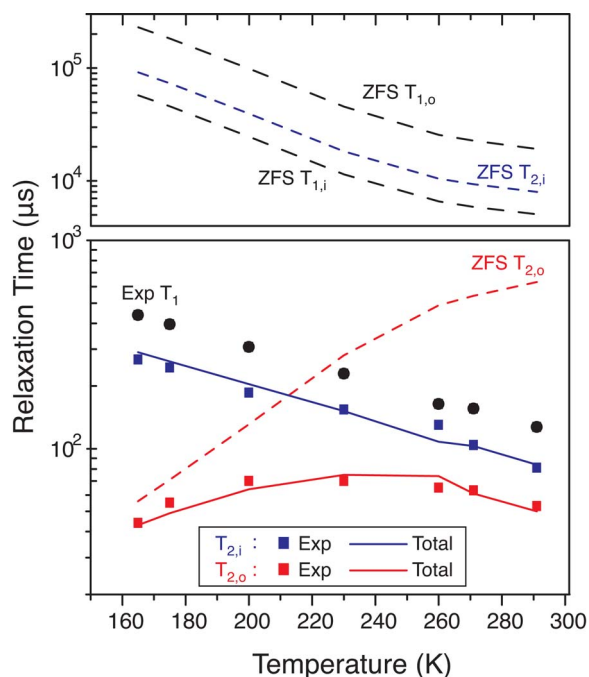
FIG. 6. Comparison of $T_2$ times for N@C$_{70}$ in CS$_2$ solution with the model described in the text. The curves labeled "ZFS" are derived from Eqs. (4)–(7). The "total" fit to $T_{2,o}$ is achieved by combining the relaxation rate from the fluctuating ZFS model, with an intrinsic decay taken to be 2/3 of $T_{2,i}$. The only free parameter in the model was a constant ZFS parameter, $D$. The contribution of the ZFS model to $T_{2,i}$ and both $T_1$ is shown to be negligible (top panel).

an Orbach relaxation mechanism, via the first excited vibrational state of the fullerene molecule. The study of electron spin relaxation in the asymmetric N@C$_{70}$ molecule permits us to distinguish this Orbach relaxation mechanism from a fluctuating ZFS mechanism. Additionally, the observation of a coherence time ($T_2$) in N@C$_{60}$ of up to 0.25 ms, the longest for any molecular electron spin, further emphasises the importance of this molecule for quantum information processing. Such times allow in excess of $10^4$ high fidelity quantum gate operations to be performed,[27] thus meeting the requirements for quantum error correction.[28]

## ACKNOWLEDGMENTS

[1] C. Knapp, K.-P. Dinse, B. Pietzak, M. Waiblinger, and A. Weidinger, Chem. Phys. Lett. **272**, 433 (1997).
[2] J. J. L. Morton, A. M. Tyryshkin, A. Ardavan, K. Porfyrakis, S. A. Lyon, and G. A. D. Briggs, J. Chem. Phys. **122**, 174504 (2005).
[3] W. Harneit, Phys. Rev. A **65**, 32322 (2002).
[4] B. R. McGarvey, J. Phys. Chem. **61**, 1232 (1957).
[5] N. Bloembergen and L. O. Morgan, J. Chem. Phys. **34**, 842 (1961).
[6] C. Knapp, N. Weiden, K. Kass, K. P. Dinse, B. Pietzak, M. Waiblinger, and A. Weidinger, Mol. Phys. **95**, 999 (1998).
[7] E. Dietel, A. Hirsch, B. Pietzak, M. Waiblinger, K. Lips, A. Weidinger, A. Gruss, and K.-P. Dinse, J. Am. Chem. Soc. **121**, 2432 (1999).
[8] J. J. L. Morton, A. M. Tyryshkin, A. Ardavan, K. Porfyrakis, S. A. Lyon, and G. A. D. Briggs (unpublished).
[9] A. D. Bokare and A. Patnaik, J. Chem. Phys. **119**, 4529 (2003).
[10] M. Kanai, K. Porfyrakis, G. A. D. Briggs, and T. J. S. Dennis, Chem. Commun. (Cambridge) 210 (2004).
[11] T. A. Murphy, T. Pawlik, A. Weidinger, M. Hohne, R. Alcala, and J. M. Spaeth, Phys. Rev. Lett. **77**, 1075 (1996).
[12] J. R. Klauder and P. W. Anderson, Phys. Rev. **125**, 912 (1962).
[13] W. B. Mims, Phys. Rev. **168**, 370 (1968).
[14] K. M. Salikhov, S. A. Dzuba, and A. M. Raitsimring, J. Magn. Reson. (1969-1992) **42**, 255 (1981).
[15] A. Carrington and G. R. Luckhurst, Mol. Phys. **8**, 125 (1964).
[16] E. W. C. Kaye and T. H. Laby, *Tables of Physical and Chemical Constants*, 15th ed. (Longmans, New York, 1986).
[17] P. W. Atkins, Adv. Mol. Relax. Processes **2**, 121 (1972).
[18] B. Chase, N. Herron, and E. Holler, J. Phys. Chem. **96**, 4262 (1992).
[19] R. Meilunas, R. P. H. Chang, S. Liu, M. Jensen, and M. M. Kappes, J. Appl. Phys. **70**, 5128 (1991).
[20] J. Menendez and J. Page, *Light Scattering in Solids VIII* (Springer, Berlin, 2000), Chap. 2.
[21] D. Kivelson, *Electron Spin Relaxation in Liquids* (Plenum, London, 1972), Chap. 10.
[22] D. Kivelson and G. Collins, Proceedings of the First International Conference on Paramagnetic Resonance, Jerusalem, 1962 (unpublished), p. 496.
[23] M. S. Dresselhaus, G. Dresselhaus, and P. C. Eklund, J. Raman Spectrosc. **27**, 351 (1996).
[24] P. Jakes, N. Weiden, R.-A. Eichel, A. Gembus, K.-P. Dinse, C. Meyer, W. Harneit, and A. Weidinger, J. Magn. Reson. **156**, 303 (2002).
[25] D. V. Khudiakov, I. V. Rubtsov, V. A. Nadtochenko, and A. P. Moravskii, Russ. Chem. Bull. **45**, 560 (1996).
[26] M. A. G. Jones, D. A. Britz, J. J. L. Morton, K. Porfyrakis, A. N. Khlobystov, A. Ardavan, and G. A. D. Briggs (unpublished).
[27] J. J. L. Morton, A. M. Tyryshkin, A. Ardavan, K. Porfyrakis, S. A. Lyon, and G. A. D. Briggs, Phys. Rev. Lett. **95**, 200501 (2005).
[28] A. Steane, Phys. Rev. A **68**, 042322 (2003).